Electronic Supplementary Material (ESI) for Journal of Materials Chemistry B.

Simple synthesis of amino acid-functionalized hydrophilic upconversion nanoparticles capped with both carboxyl and amino groups for bimodal imaging

Gui-Mei Han,[a] Hong-Xin Jiang,[a] Yan-Fang Huo,[a] De-Ming Kong*[a, b]

[a]State Key Laboratory of Medicinal Chemical Biology, Tianjin Key Laboratory of Biosensing and Molecular Recognition, College of Chemistry, Nankai University, Tianjin, 300071, P. R. China.

[b]Collaborative Innovation Center of Chemical Science and Engineering (Tianjin), Tianjin, 300071, P. R. China

* Corresponding author. Tel.: +86-22-23500938; Fax: +86-22-23502458

E-mail address: kongdem@nankai.edu.cn (D.-M. Kong).

1. Synthesis of the rare-earth stearate precursors

1.1 Synthesis of the rare-earth stearate $(C_{17}H_{35}COO)_3RE$ (RE= $Lu_{0.78}Yb_{0.20}Er_{0.02}$)

The rare-earth stearate $(C_{17}H_{35}COO)_3RE$ (RE = $Lu_{0.78}Yb_{0.20}Er_{0.02}$) was synthesized according to the literature.[1] Typically, $Lu(NO_3)_3·6H_2O$ (0.78 mmol, 0.7318 g), $Yb(NO_3)_3·5H_2O$ (0.2 mmol, 0.1796 g), $Er(NO_3)_3·6H_2O$ (0.02 mmol, 0.0185 g) and steric acid (6 mmol, 1.7069 g) were dissolved in 50 mL ethanol by stirring at 78 ^oC until a transparent solution was obtained. Then, 10 mL water containing 8 mmol NaOH (0.2380 g) was added dropwise and the mixture was refluxed for 40 min. Subsequently, the product, obtained from filtering by a microporous membrane, was washed by ethanol, and then dried at 60 ^oC for 12 h.

1.2 Synthesis of the rare-earth stearate $(C_{17}H_{35}COO)_3RE$ (RE= $Lu_{0.55}Gd_{0.24}Yb_{0.20}Tm_{0.01}$)

The precursor $(C_{17}H_{35}COO)_3RE$ (RE = $Lu_{0.55}Gd_{0.24}Yb_{0.20}Tm_{0.01}$) was synthesized in the same way as above, except that $Lu(NO_3)_3·6H_2O$ (0.78 mmol, 0.7318 g), $Yb(NO_3)_3·5H_2O$ (0.2 mmol, 0.1796 g), $Er(NO_3)_3·6H_2O$ (0.02 mmol, 0.0185 g) were replaced by $Lu(NO_3)_3·6H_2O$ (0.55 mmol, 0.5160 g), $Gd(NO_3)_3·6H_2O$ (0.24 mmol, 0.2166 g), $Yb(NO_3)_3·5H_2O$ (0.2 mmol, 0.1796 g) and $Tm(NO_3)_3·6H_2O$ (0.01 mmol, 0.0089 g).

2. Optimization of synthesis conditions

In order to obtain UCNPs with more regular morphology and more excellent luminescent properties, we optimized the reaction conditions, including the ratio of the reactants, reaction temperature and time. We used the aspartate-functionalized $NaLuF_4$:Yb/Er (Asp-$NaLuF_4$: Yb/Er) as an example to explore the best reaction conditions.

First of all, optimal ratio between rare-earth stearate precursor $(C_{17}H_{35}COO)_3RE$ and NH_4F was tested by keeping $(C_{17}H_{35}COO)_3RE$ at 0.3832 g but varying NH_4F concentration. The results of XRD showed when a RE^{3+}/F^- molar ratio of 1:2.5 was

used, the synthesized Asp-$NaLuF_4$:Yb/Er UCNPs existed as a mixture of α and β phases (Fig. S1). With the increase of RE^{3+}/F^- molar ratio, a phase transformation was observed. That is, when the RE^{3+}/F^- molar ratio was changed to 1:4 or 1:6, the synthesized Asp-$NaLuF_4$:Yb/Er UCNPs existed as pure β phase. In addition, the Asp-$NaLuF_4$:Yb/Er UCNPs synthesized using the RE^{3+}/F^- molar ratio of 1:4 gave the highest upconversion luminescence (UCL) intensity (Fig. S2). As a result, the optimal RE^{3+}/F^- molar ratio was selected as 1:4.

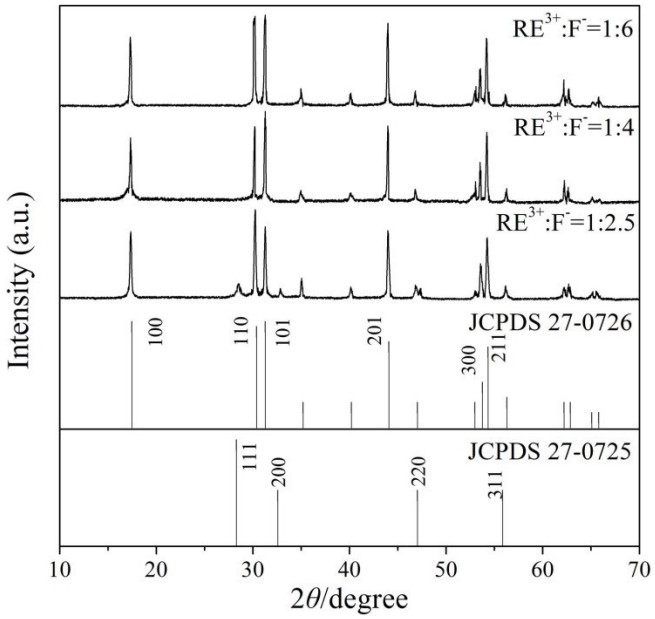

Fig. S1 XRD patterns of the Asp-$NaLuF_4$:Yb/Er UCNPs synthesized using different RE^{3+}/F^- molar ratios.

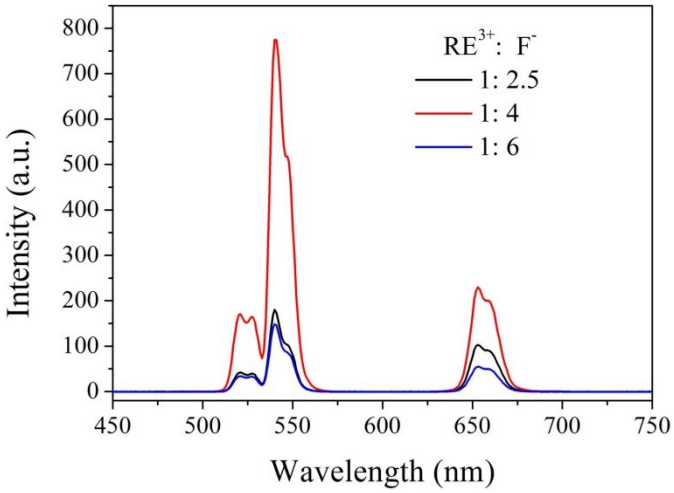

Fig. S2 UCL spectra of the Asp-$NaLuF_4$:Yb/Er UCNPs synthesized using different RE^{3+}/F^- molar ratios

Then, optimal hydrothermal reaction temperature was tested. The XRD patterns showed that the Asp-$NaLuF_4$:Yb/Er UCNPs synthesized at 150 ^oC were composed of mixed α and β phases (Fig. S3). With the increase of reaction temperature, the proportion of α phase decreased and a pure β phase was obtained at 200 ^oC. Correspondingly, the synthesized Asp-$NaLuF_4$:Yb/Er gave a significantly increased upconversion luminescence (UCL) intensity with the increase of hydrothermal temperature from 150 ^oC to 180 ^oC (Fig. S4). When the temperature was further increased to 200 ^oC, the increase of luminescence intensity could still be observed. The increasing rate, however, was remarkably reduced. Given high temperature might lead to the decomposition of amino acids, 200 ^oC was used in the following experiments.

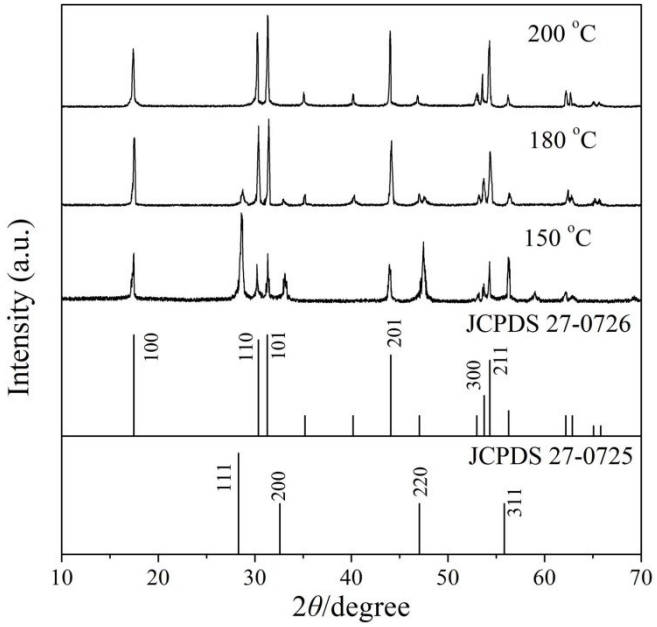

Fig. S3 XRD patterns of the Asp-$NaLuF_4$:Yb/Er UCNPs synthesized under different hydrothermal temperatures.

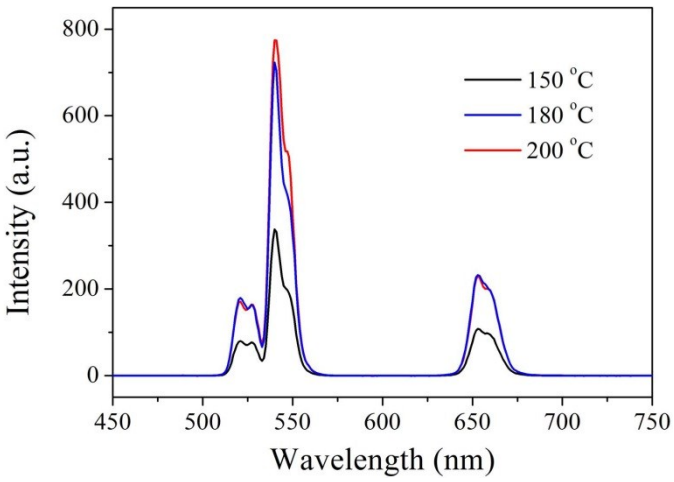

Fig. S4 UCL spectra of the Asp-$NaLuF_4$:Yb/Er UCNPs synthesized under different hydrothermal temperatures

Finally, optimal hydrothermal reaction time was investigated. With the increase of reaction time, a phase transformation was also observed from α, β-mixed phase to a pure β phase (Fig. S5). When the reaction time was extended to 24 h, Asp-$NaLuF_4$:Yb/Er with pure β phase could be obtained. Correspondingly, the upconversion luminescent intensity of synthesized Asp-$NaLuF_4$:Yb/Er increased with reaction time (Fig. S6). As a compromise between reaction time and luminescent intensity, 24 h was selected for the following experiments.

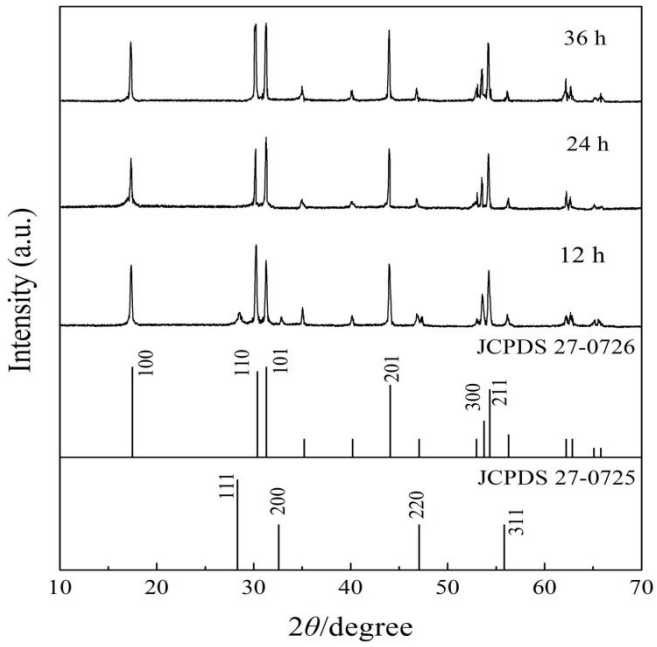

Fig. S5 XRD patterns of the Asp-$NaLuF_4$:Yb/Er UCNPs synthesized with different hydrothermal time

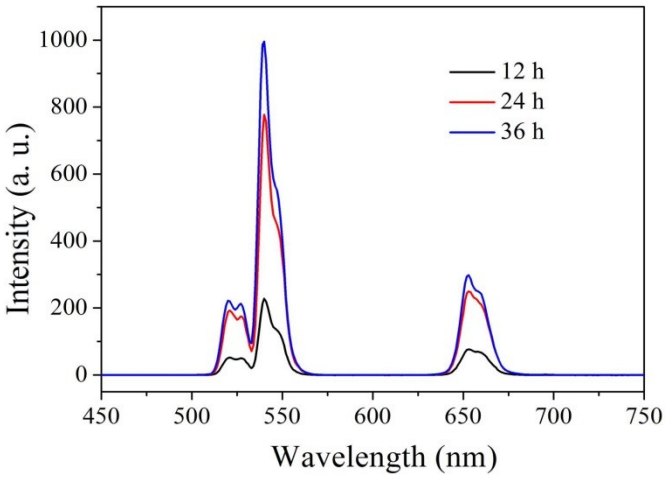

Fig. S6 UCL spectra of the Asp-$NaLuF_4$:Yb/Er UCNPs synthesized with different hydrothermal time.

3. Anti-photobleching abilities of the amino acid-functionalized UCNPs

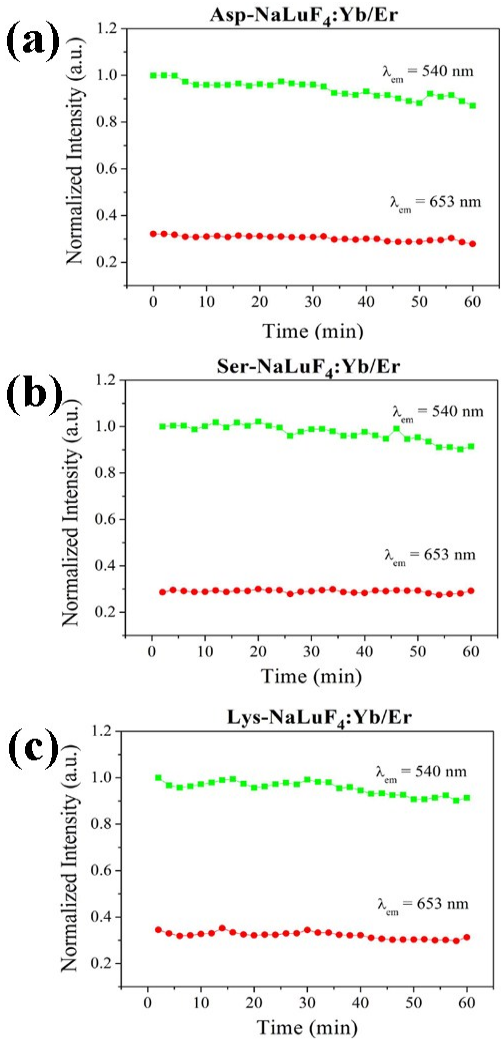

Fig. S7 UCL intensity of the prepared amino acid-functionalized UCNPs as a function of illumination time under excitation of 980 nm laser

4. ^{1}H-NMR characterization of the synthesized Asp-NaLuF$_4$:Yb/Er UCNPs

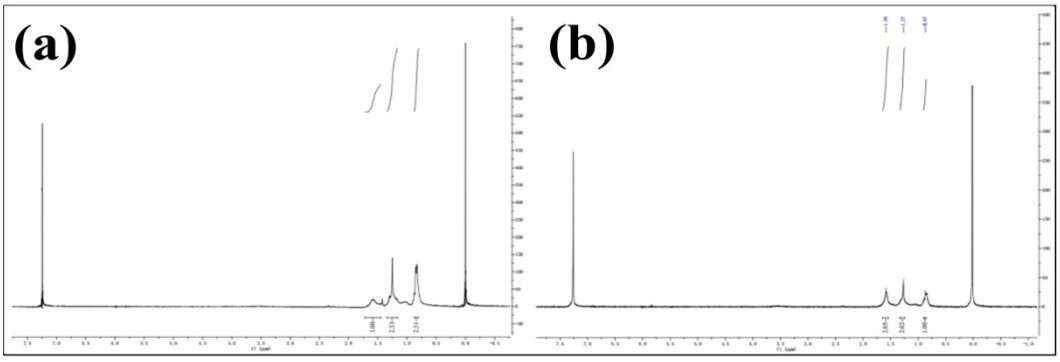

Fig. S8 ^{1}H-NMR of (a) the synthesized Asp-NaLuF$_4$:Yb/Er UCNPs and (b) free aspartic acid in $CDCl_3$, ^{1}H-NMR (300 MHz, $CDCl_3$), δ = 1.29 (d, J = 11.3 Hz, 2H), 0.87 (s, 1H).

5. Conjugation of Ser-NaLuF$_4$:Yb/Er with amino or carboxyl-functionalized fluorescent-labelled oligonucleotides

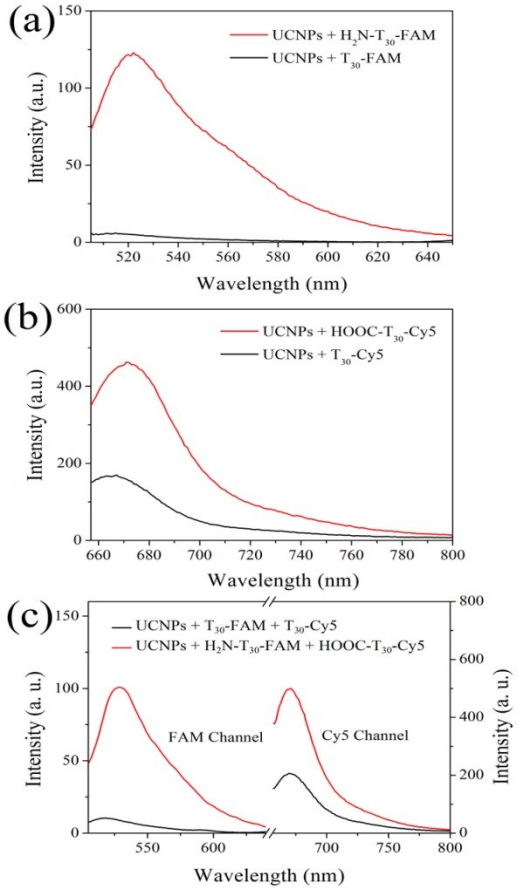

Fig. S9 Fluorescence signal of FAM or/and Cy5 emitted by Ser-NaLuF$_4$:Yb/Er after conjugation with (a) H_2N-T_{30}-FAM, (b) HOOC-T_{30}-Cy5, (c) both H_2N-T_{30}-FAM and HOOC-T_{30}-Cy5. T_{30}-FAM and T_{30}-Cy5 are used as controls. The excitation wavelengths of FAM and Cy5 are 495 and 649 nm, respectively.

6. Conjugation of Lys-$NaLuF_4$:Yb/Er with amino or carboxyl-functionalized fluorescent-labelled oligonucleotides

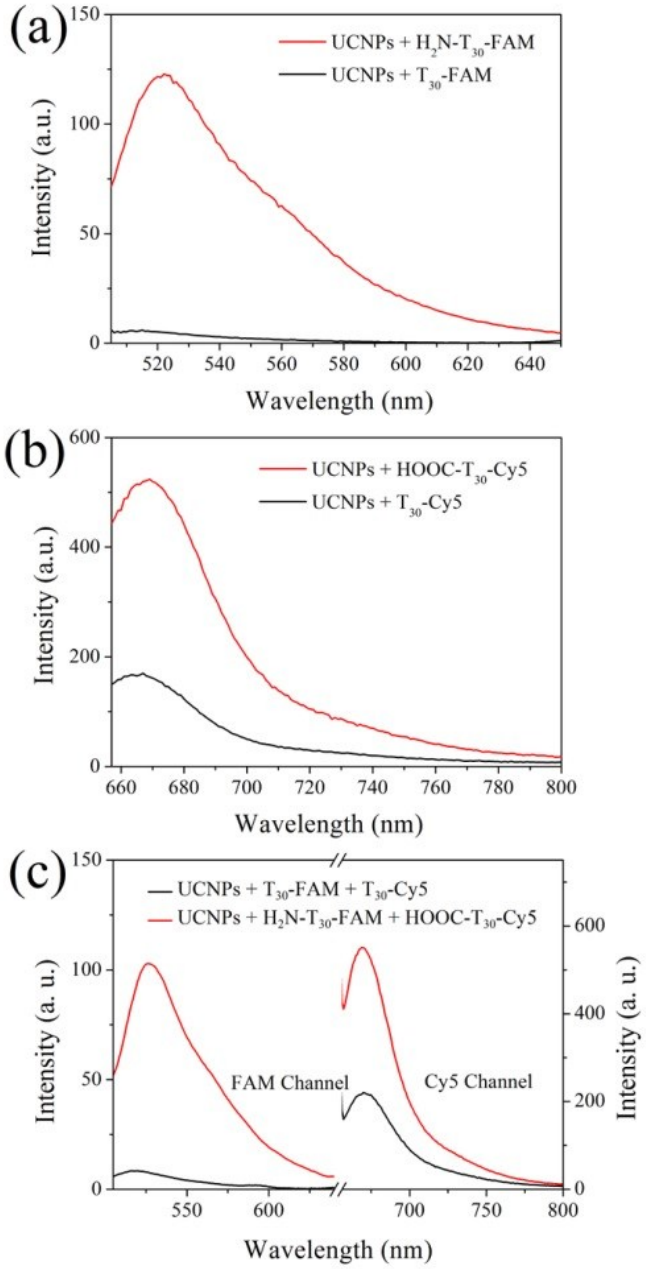

Fig. S10 Fluorescence signal of FAM or/and Cy5 emitted by Lys-$NaLuF_4$:Yb/Er after conjugation with (a) H_2N-T_{30}-FAM, (b) HOOC-T_{30}-Cy5, (c) both H_2N-T_{30}-FAM and HOOC-T_{30}-Cy5. T_{30}-FAM and T_{30}-Cy5 are used as controls. The excitation wavelengths of FAM and Cy5 are 495 and 649 nm, respectively.

7. Characterization of the Asp-$NaLuF_4$:Gd/Yb/Tm UCNPs

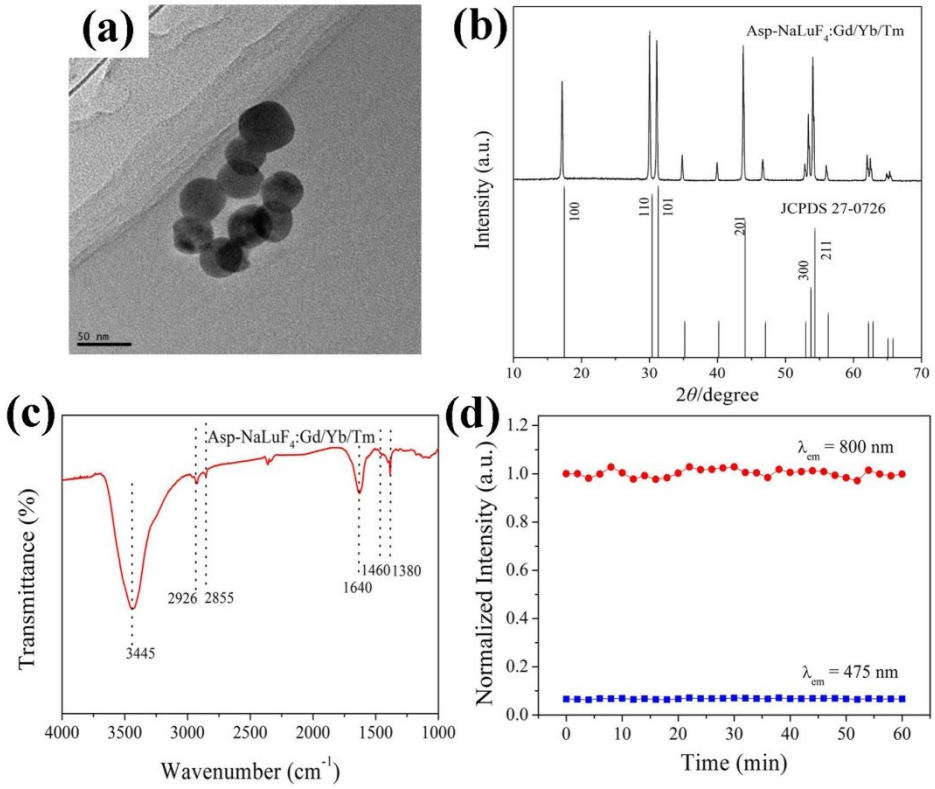

Fig. S11 Characterization of the prepared Asp-$NaLuF_4$:Gd/Yb/Tm UCNPs. (a) TEM, (b) XRD patterns, (c) FT-IR spectra and (d) anti-photobleaching ability of Asp-$NaLuF_4$:Gd/Yb/Tm UCNPs.

8. Conjugation of Asp-$NaLuF_4$:Gd/Yb/Tm with amino or carboxyl-functionalized fluorescent-labelled oligonucleotides

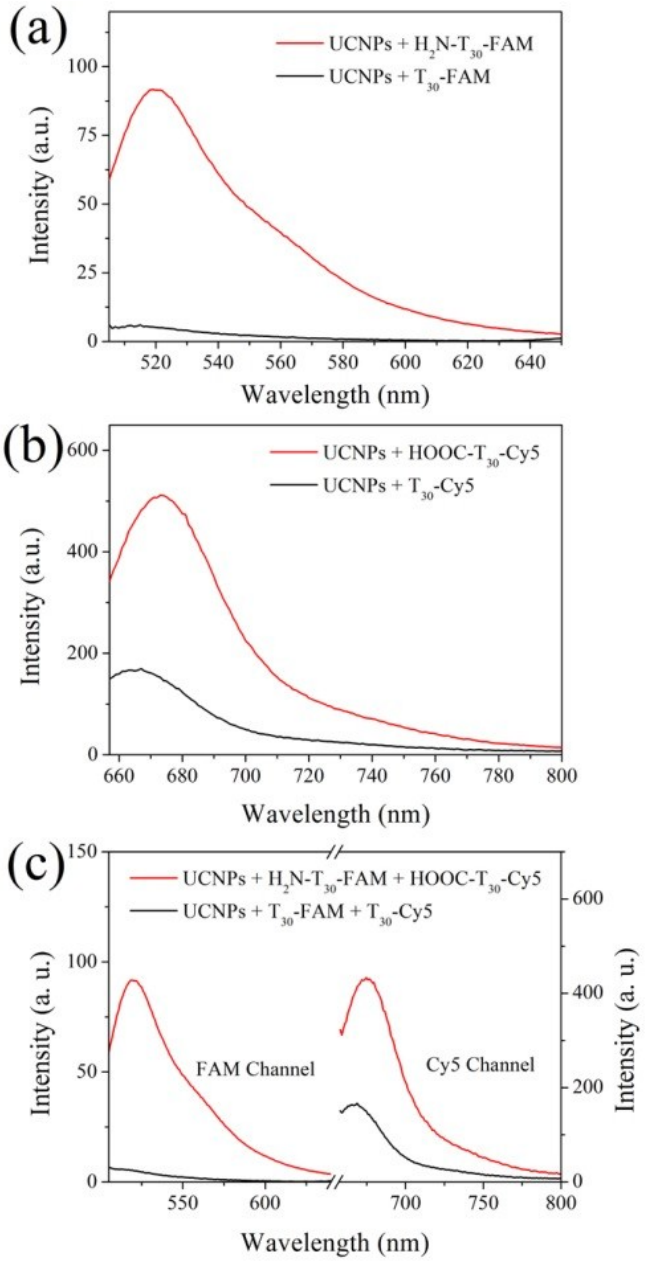

Fig. S12 Fluorescence signal of FAM or/and Cy5 emitted by Asp-$NaLuF_4$:Gd/Yb/Tm after conjugation with (a) H_2N-T_{30}-FAM (b) HOOC-T_{30}-Cy5 (c) both H_2N-T_{30}-FAM and HOOC-T_{30}-Cy5. T_{30}-FAM and T_{30}-Cy5 are used as controls. The excitation wavelengths of FAM and Cy5 are 495 and 649 nm, respectively.

Reference

[1] M. Wang, C. C. Mi, W. X, Wang, C. H. Liu, Y. F. Wu, Z. R. Xu, C. B. Mao and S. K. Xu, *ACS Nano,* 2009, **3**, 1580-1586.